Digital Innovations & Contemporary Research in SCIENCE, ENGINEERING & TECHNOLOGY
Vol. 5 No. 4. December. 2017

Article Citation Format
B.O. Falodun & S.A. Amoo (2017). Analysis of Unsteady Casson Fluid Flow Past a Semi- infinite Vertical Porous Plate Under the influence of Thermo-diffusion and Diffusion-thermo. Journal of Digital Innovations & Contemp Res. In Sc., Eng & Tech. Vol. 5, No. 4. Pp 23-44.

Article Progress Time Stamps

Article Type: Research Article
Manuscript Received: 11nd November, 2017
Review Type: Blind
Final Acceptance:: 15th December, 2017
DOI Prefix: 10.22624

Analysis of Unsteady Casson Fluid Flow Past a Semi- infinite Vertical Porous Plate Under the influence of Thermo-diffusion and Diffusion-thermo

B.O. Falodun
[1]Department of Mathematics
University of Ilorin
Ilorin, Nigeria
Email: falodunbidemi2014@gmail.com

S. A. Amoo
Department of Mathematics and Statistics
Federal University Wukari
Wukari, Nigeria
Email: drsikiruamoo@gmail.com

ABSTRACT

The paper investigated the effects of thermo-diffusion and diffusion-thermo on unsteady Casson fluid flow past a semi-infinite vertical porous plate with magnetic field and chemical reaction. Our governing equations are set of coupled partial differential equations subject to time dependent boundary conditions were transformed into a dimensionless form by introducing an appropriate set of non-dimensional quantities and solved using Spectral Relaxation Method (SRM). Effects of all the flow parameters on the velocity, temperature and concentration profiles were plotted in graphs. Also, effects of flow parameters on the local skin friction, local Nusselt number and Sherwood number are presented in tabular form. The results obtained with SRM were compared with existing result in literature and were found in excellent agreement. It was discoved that increasing the permeability parameter (λ) decreased the velocity profile. It was revealed that an increase in Casson parameter (β) reduced the velocity profile.

Keywords*:* Unsteady, Vertical Plate, Thermo-diffusion, Diffusion-thermo, Porous Medium Spectral Relaxation Method

1. INTRODUCTION

Non-Newtonian fluid finds application in industry and technology. Despite the importance of non-Newtonian fluids in industry and technology little attention has been paid on the unsteady characteristics of this type of fluid due to their complexity. Casson fluid is an example of non-Newtonian fluid. Casson fluid can be defined as a shear thinning liquid which is assumed to have an infinite viscosity at zero rate of shear, a yield stress below which no flow occurs and a zero viscosity at an infinite rate of shear. Examples of casson fluid are; honey, soup, etc and human blood can be treated as a casson fluid. Within last few years, Pushpalatha *et al* (2011) investigated numerical study of chemically reacting unsteady casson fluid past a stretching surface with cross diffusion and thermal radiation. Computational analysis of magnetohydrodynamics casson and maxwell flows over a stretching sheet with cross diffusion were investigated by Kumaran *et al* (2017). In another research, Srinivasa (2016) studied numerical treatment of casson fluid free convective flow past an infinite vertical plate filled in presence of thermal radiation:A finite element techniques. Several authors like Emmanuel *et al* (2015) Animasaun *et al* (2016); Monica *et al* (2016); Animasaun (2016); Pramanik (2016); Muhammad (2016); Falodun and Amoo (2017) just to mention a few have discussed extensively the flow of casson Non-Newtonian fluid.

Heat and mass transfer is of great importance in many engineering processes. As a matter of fact, heat and mass transfer occurs independent from each other. Wherever heat and mass transfer simultaneously in a moving fluid the relations between the energy fluxes and the driving potentials are complicated. Diffusion thermal or Dufour effect is the energy flux caused by composition gradient while thermal diffusion or Soret effect is the mass flux created by temperature gradient. The effects of diffusion-thermo and thermo-diffusion can not be neglected when the thermal and concentration gradients are at a high temperature. Alao *et al* (2016) investigated the effects of thermal radiation, Soret and Dufour on an unsteady heat and mass transfer flow of a chemically reacting fluid past a semi-infinite vertical plate with viscous dissipation. Yanala and Vempati (2016) recently studied numerical solution of thermo-diffusion and diffusion-thermo effects on unsteady MHD free convective mass transfer flow past an infinite vertical porous plate with oscillatory suction velocity. Rallabandi (2016) studied combined influence of thermal diffusion and diffusion thermo on unsteady MHD free convective fluid flow past an infinite vertical porous plate in presence of chemical reaction. Bhavana *et al* (2013) studied the soret effect on free convective unsteady MHD flow over a vertical plate with heat source. Mohammed and Suneetha (2016) discussed influence of thermo-diffusion and heat source on MHD free convective radiating dissipative boundary layer of chemically reacting fluid flow in a porous vertical surface.

Prakash *et al* (2015) have studied thermo-diffusion and chemical reaction effects on MHD three dimensional free convective Couette flow. Mashan Rao *et al* (2013) studied chemical reaction and hall effects on MHD convective flow along an infinite vertical porous plate with variable suction and heat absorption. Vidyasagar *et al* (2015) had studied unsteady MHD free convection flow of a viscous dissipative Kuvshinski fluid past an infinite vertical porous plate in the presence of radiation, thermal diffusion and chemical effects. Kishore *et al* (2014) investigated the effect of chemical reaction on MHD free convection flow of dissipative fluid past an exponentially accelerated vertical plate. Shivaiah and Anand (2012) studied chemical reaction effect on an unsteady MHD free convection flow past a vertical porous plate in the presence of suction or injection. Sulochana *et al* (2016) studied numerical investigation of chemically reacting MHD flow due to a rotating cone with thermophoresis and Brownian motion.

Our aim in this paper is to present the numerical analysis of unsteady casson fluid flow past a semi-infinite vertical porous plate with the use of SRA. To the best of our knowledge, the authors were not aware of article in literature that had reported thermo-diffusion and diffusion-thermo effects on unsteady casson fluid flow past a semi-infinite vertical porous plate with magnetic field and chemical reaction. As a result of this,

our focus in this article is to discuss extensively how to use spectral relaxation method (SRM) to solve the model under investigation and discuss the influence of all pertinent flow parameters involved in the equations. In implementing the SRM, a symbolic mathematical software MATLAB is used.

2. PROBLEM FORMULATION

This research article considered an unsteady two-dimensional, laminar boundary layer flow. Our focus is to investigate thermo-diffusion and diffusion-thermo effects on unsteady casson fluid flow past a semi-infinite vertical porous plate with magnetic field and chemical reaction (see Rao et al.[21]). This problem involves two coordinate (x^*, y^*) because we are considering a two-dimensional problem. The coordinate x^*-axis is considered along the vertical infinite plate while the coordinate y^*-axis is normal to the plate as shown in **figure 1**. The initial time of flow is at $t^* = 0$. All physical variables are assumed to be the function of t^* and y^* respectively. The porous medium hole is assumed to be very small and the influence of Soret and Dufour are considered to be significant.

With all the assumptions above and the application of the Boussinesq's approximation, the governing boundary layer equations becomes:

$$\frac{\partial v^*}{\partial y^*} = 0, \quad (1)$$

$$\frac{\partial u^*}{\partial t^*} + v^* \frac{\partial u^*}{\partial y^*} = v\left(1 + \frac{1}{\beta}\right)\frac{\partial^2 u^*}{\partial y^{*2}} + g\beta_t(T - T_0) + g\beta_c(C - C_0) - \frac{\sigma\beta_0^2 u^*}{\rho} - \frac{v}{k^*}u^*, \quad (2)$$

$$\frac{\partial T}{\partial t^*} + v^* \frac{\partial T}{\partial y^*} = \alpha \frac{\partial^2 T}{\partial y^{*2}} - \frac{1}{\rho c_p}\frac{\partial q_r}{\partial y^*} + \frac{\mu}{\rho c_p}\left(\frac{\partial u^*}{\partial y^*}\right)^2 + \frac{D k_T}{C_s c_p}\frac{\partial^2 C}{\partial y^{*2}} \quad (3)$$

$$\frac{\partial C}{\partial t^*} + v^* \frac{\partial C}{\partial y^*} = D \frac{\partial^2 C}{\partial y^{*2}} + \frac{D K_T}{T_m}\left(\frac{\partial^2 T}{\partial y^{*2}}\right) - K_r^*(C - C_0). \quad (4)$$

subject to the boundary conditions

$$u^* = U_0 \quad , T = T_w + \psi(T_w - T_0)exp(n^* t^*) \quad , C = C_w + \psi(C_w - C_0)exp(n^* t^*) \quad at \quad y^* = 0 \quad (5)$$

$$u^* \to 0 \quad , T \to T_0 \quad , C \to C_0 \quad as \quad y^* \to \infty \quad (6)$$

In equation (1), we have $v^* = constant$ when we integrate. The suction velocity at the plate is a constant and in this article we assumed it to be the combination of both constant and function of time given as:

$$v^* = -\gamma_0(1 + \xi A exp(n^* t^*)) \quad (7)$$

where v^*, u^* is the Velocity components in x^* and y^* directions, g is the Acceleration due to gravity ,T is Temperature of the fluid, C is Specie Concentration, C_0 is Free stream concentration, k^* is Permeability term, t^* is Time , c_p is Specific heat at constant pressure, D is Mass Diffusivity, k_T is Thermal diffusion ratio, c_s is Concentration susceptibility, T_m is Mean fluid temperature, K_r^* is Chemical reaction parameter, T_0 is Free stream temperature, v is Fluid viscosity, β is Non-Newtonian casson parameter, β_t is Thermal expansion coefficient, β_c is Concentration expansion coefficient, σ is Electrical conductivity, β_0 is Magnetic field strength, ρ is Fluid density, α is Thermal diffusivity, μ is kinematic viscosity

From equation (2), the term $v(1+\frac{1}{\beta})\frac{\partial^2 u^*}{\partial y^{*2}}$ is the viscous term where β is the casson parameter, $g\beta_t(T-T_0)$ and $g\beta_c(C-C_0)$ are thermal and concentration buoyancy, $\frac{\sigma\beta_0^2 u^*}{\rho}$ is magnetic field term, this term is negative because the magnetic field strenght β_0 is applied opposite to the flow while $\frac{v}{k^*}u^*$ is the permeability term.

Also in equation (3), $\alpha\frac{\partial^2 T}{\partial y^{*2}}$ is the diffusion term where the thermal diffusivity α is expressed as $\alpha=\frac{k}{\rho c_p}$, also $\frac{1}{\rho c_p}\frac{\partial q_r}{\partial y^*}$ is the radiative heat flux. The radiative heat flux in the x^*-direction $(\frac{\partial q_r}{\partial x^*})$ is neglected in this article. The term $\frac{\mu}{\rho c_p}(\frac{\partial u^*}{\partial y^*})^2$ and $\frac{D k_T}{C_s c_p}\frac{\partial^2 C}{\partial y^{*2}}$ are the viscous dissipation term and Dufour term respectively.

Finally, equation (4) is the specie concentration equation and $D\frac{\partial^2 C}{\partial y^{*2}}$ is the mass diffusion term, $\frac{DK_T}{T_m}(\frac{\partial^2 T}{\partial y^{*2}})$ and $K_r^*(C-C_0)$ are the Soret and chemical reaction term. Following Hayat et al.[22], the rheologocal equation of an isotropic and incompressible flow of non-Newtonian Casson fluid flow is given by:

$$\tau_{ij}=(\mu_B+\frac{P_y}{\sqrt{2\pi}})2e_{ij} \quad when \quad \pi>\pi_c \qquad (8)$$

$$\tau_{ij}=(\mu_B+\frac{P_y}{\sqrt{2\pi}})2e_{ij} \quad when \quad \pi>\pi_c \qquad (9)$$

where the yield stress P_y is expressed as $P_y=\frac{\mu_B\sqrt{2\pi}}{B}$, μ_B is plastic dynamic viscosity and π is the product of component of deformation rate with itself meaning that $\pi=e_{ij}e_{ij}$ Simplifying the radiative heat flux using the Roseland approximation as described by Adegbie and Fagbade [23] and reported in Alao et al.[10] that;

$$q_r=\frac{4\sigma_s}{3k_e}\frac{\partial T^4}{\partial y^*} \qquad (10)$$

Using the application of Roseland approximation, this study is restricted only to an optically thin fluid. Assuming that the temperature difference within the flow is small and linearizing equation (10) by expanding T^4 with Taylor series about T_0 and neglect the higher order term to give

$$T^4=4T_0^3T-3T_0^4 \qquad (11)$$

Introducing the following non-dimensional quantities in other to write the governing equations and the boundary conditions in a dimensionless form;

$$u=\frac{u^*}{u_0},\quad y=\frac{v_0^2 t^*}{v},\quad t=\frac{v_0^2 t^*}{v},\quad n=\frac{vn^*}{v_0^2},\quad \theta=\frac{T-T_0}{T_W-T_0},\quad \lambda=\frac{v}{u_0 k^*},\quad Sr=\frac{Dk_T(T_W-T_0)}{T_m v(C_W-C_0)} \qquad (12)$$

$$\phi=\frac{C-C_0}{C_W-C_0},\quad Pr=\frac{v\rho c_p}{k}=\frac{v}{\alpha},\quad Sc=\frac{v}{D},\quad Gr=\frac{g\beta_t v(T_W-T_0)}{u_0 v_0^2},\quad Gm=\frac{g\beta_c v(C_W-C_0)}{u_0 v_0^2} \qquad (13)$$

$$Ec=\frac{u_0^2}{c_p(T_W-T_0)},\quad k_r^2=\frac{k_r^* v}{v_0^2},\quad Nr=\frac{16\sigma_s T_\infty^3}{3k_e k},\quad M=\frac{\sigma\beta_0^2 v}{\rho v_0^2},\quad Du=\frac{D k_T(C_W-C_0)}{c_s c_p v(T_W-T_0)} \qquad (14)$$

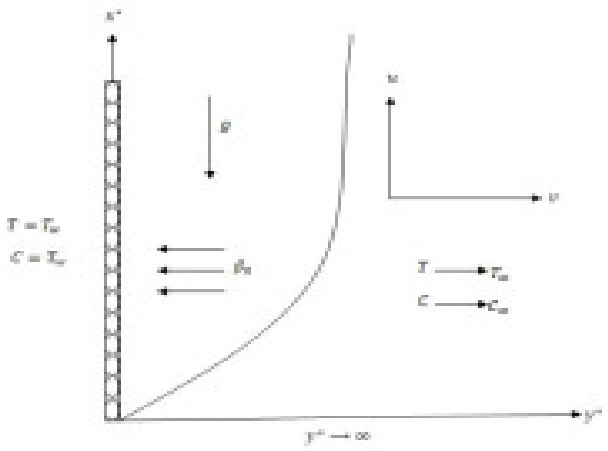

Figure 1: Physical Interpretation of the Problem

substituting equations. (12)-(14) into equations (2)-(4) gives the dimensionless form of equations below;

$$\frac{\partial u}{\partial t} - \alpha\frac{\partial u}{\partial y} - (1+\frac{1}{\beta})\frac{\partial^2 u}{\partial y^2} - G_r\theta - G_m\phi + (\lambda + M)u = 0 \tag{15}$$

$$\frac{\partial \theta}{\partial t} - \alpha\frac{\partial \theta}{\partial y} - (\frac{1+Nr}{P_r})\frac{\partial^2 \theta}{\partial y^2} - E_c(\frac{\partial u}{\partial y})^2 - D_u(\frac{\partial^2 \phi}{\partial y^2}) = 0 \tag{16}$$

$$\frac{\partial \phi}{\partial t} - \alpha\frac{\partial \phi}{\partial y} - \frac{1}{S_c}\frac{\partial^2 \phi}{\partial y^2} - S_r\frac{\partial^2 \theta}{\partial y^2} + k_r^2\phi = 0 \tag{17}$$

The dimensionless initial and boundary conditions are;

$$u = 1,\ \theta = 1 + \varepsilon e^{nt},\ \ \phi = 1 + \varepsilon e^{nt} \text{ at } y = 0 \tag{18}$$

$$u \to 0,\ \theta \to 0,\ \phi \to 0,\ \text{at } y \to \infty \tag{19}$$

where $\alpha = -(1 + \xi exp(nt))$, β is the casson parameter, Gr is the thermal Grashof number, Gm is the modified Grashof number, λ is the permeability parameter, M is the magnetic parameter, Nr is the thermal radiation parameter, Pr is the Prandtl number, Ec is the Eckert number, Du is the Dufour number, Sc is the Schmidt number, Sr is the Soret number, and k_r is the chemical reaction parameter.

The important physical parameters are the local skin friction, local Nusselt number and local Sherwood number. In a non-dimensional form, the local skin friction at the plate is expressed as:

$$C_f = \frac{\tau_W}{\rho U_0 V_0} \quad where \quad \tau_W = (\mu_B + \frac{P_y}{\sqrt{2\pi}})\frac{\partial u}{\partial y}|_{y=0} \tag{20}$$

τ_w is the local skin friction or shear stress at the plate. Using the non-dimensional qunatities on equation (18) and simplify to obtain:

$$\sqrt{Re_x}C_f = (1+\frac{1}{\beta})f''(0) \quad (21)$$

Rate of heat transfer coefficient in a non-dimensional form with respect to Nusselt number is given by:

$$Nu = -x\frac{(\frac{\partial T}{\partial y^*})_{y^*=0}}{T_w - T_\infty} \quad (22)$$

This implies that:

$$NuRe_x^{-1} = -(\frac{\partial \theta}{\partial y})_{y=0}$$

Finally, the rate of mass transfer coefficient in a non-dimensional form withh respect to the local Sherwood number is given by:

$$Sh = -x\frac{(\frac{\partial C}{\partial y^*})_{y^*=0}}{C_w - C_\infty} \quad (23)$$

This implies that:

$$ShRe_x^{-1} = -(\frac{\partial \phi}{\partial y})_{y=0}$$

where the local Reynolds number Re_x is expressed as $\frac{V_0 x}{\nu}$

3. NUMERICAL TECHNIQUE

In this article, a numerical method called spectral relaxation method (SRM) is employed in solving the transformed partial differential equations. SRM adopt the relaxation type of Gauss-Siedel by linearizing and decoupling the system of nonlinear differential equations, see Motsa[24]. In the application of SRM, linear terms in the equation is evaluated at the current iteration level denoted by $r+1$ and the nonlinear terms is assumed to be known at previous iteration level denoted by r. Chebyshev spectral collocation method is used in integrating the sequence of equations. Using the SRM on the transformed governing equations we have

$$\beta\frac{\partial u_{r+1}}{\partial t} = a_{0,r}u'_{r+1} + a_{1,r}u''_{r+1} + a_{2,r} + a_{3,r}u_{r+1} \quad (24)$$

$$Pr\frac{\partial \theta_{r+1}}{\partial t} = e_{0,r}\theta'_{r+1} + e_{1,r}\theta''_{r+1} + e_{2,r} + e_{3,r} \quad (25)$$

$$Sc\frac{\partial \phi_{r+1}}{\partial t} = f_{0,r}\phi'_{r+1} + \phi''_{r+1} + f_{1,r} - k_r^2\phi_{r+1} \quad (26)$$

with the boundary conditions:

$$u_{r+1}(0,t) = 1, \quad u_{r+1}(\infty,t) = 0, \quad \theta_{r+1}(0,t) = 1 + \xi exp(nt) \tag{27}$$

$$\theta_{r+1}(\infty,t) = 0, \quad \phi_{r+1}(0,t) = 1 + \xi exp(nt), \quad \phi_{r+1}(0,t) = 0 \tag{28}$$

The following initial approximation is choosen to satisfy the boundary conditions

$$u_0(y,t) = exp(-y), \quad \theta_0(y,t) = \phi_0(y,t) = exp(-y) + \xi exp(nt) \tag{29}$$

The coefficient parameters $d_{0,r}, d_{1,r}, d_{2,r}, d_{3,r}, e_{0,r}, e_{1,r}, e_{2,r}, e_{3,r}, f_{0,r}, f_{1,r}$ are as follows

$$d_{0,r} = -\alpha\beta, \quad d_{1,r} = (1+\beta), \quad d_{2,r} = Gr\theta_r + Gc\phi_r, \quad d_{3,r} = -(\lambda + M), \quad e_{0,r} = -\alpha Pr$$
$$e_{1,r} = (1 + Nr), \quad e_{2,r} = PrEc(u'_{r+1})^2, \quad e_{3,r} = PrDu\phi''_r, \quad f_{0,r} = -Sc\alpha, \quad f_{1,r} = ScSr\theta''_{r+1}$$

Using equation (29), equations (24)-(28) are solved iteratively. Chebyshev spectral collocation method is used to discretize equations (24)-(28) in t-direction and implicit finite difference method will be apply in y-direction. Applying the spectral method on (24)-(28) to obtain

$$\beta \frac{du_{r+1}}{dt} = (d_{0,r}D + d_{1,r}D^2 + d_{3,r})u_{r+1} + d_{2,r} \tag{30}$$

$$Pr \frac{d\theta_{r+1}}{dt} = (e_{0,r}D + e_{1,r}D^2)\theta_{r+1} + e_{2,r} + e_{3,r} \tag{31}$$

$$Sc \frac{d\phi_{r+1}}{dt} = (f_{0,r}D + D^2 - k_r^2)\phi_{r+1} + f_{1,r} \tag{32}$$

and

$$u_{r+1} = \begin{bmatrix} u_{r+1}(x_0,t) \\ u_{r+1}(x_1,t) \\ \vdots \\ u_{r+1}(x_{N_x-1},t) \\ u_{r+1}(x_{N_x},t) \end{bmatrix}, \; d_{0,r} = \begin{bmatrix} d_{0,r}(x_0,t) & & & \\ & d_{0,r}(x_1,t) & & \\ & & \ddots & \\ & & & d_{0,r}(x_{N_x},t) \end{bmatrix} \tag{33}$$

$$\theta_{r+1} = \begin{bmatrix} \theta_{r+1}(x_0,t) \\ \theta_{r+1}(x_1,t) \\ \vdots \\ \theta_{r+1}(x_{N_x-1},t) \\ \theta_{r+1}(x_{N_x},t) \end{bmatrix}, \; e_{1,r} = \begin{bmatrix} e_{0,r}(x_0,t) & & & \\ & e_{0,r}(x_1,t) & & \\ & & \ddots & \\ & & & e_{0,r}(x_{N_x},t) \end{bmatrix} \tag{34}$$

$$\phi_{r+1} = \begin{bmatrix} \phi_{r+1}(x_0,t) \\ \phi_{r+1}(x_1,t) \\ \vdots \\ \phi_{r+1}(x_{N_x-1},t) \\ \phi_{r+1}(x_{N_x},t) \end{bmatrix}, \; f_{0,r} = \begin{bmatrix} f_{0,r}(x_0,t) & & & \\ & f_{0,r}(x_1,t) & & \\ & & \ddots & \\ & & & f_{0,r}(x_{N_x},t) \end{bmatrix} \tag{35}$$

We proceed to apply finite difference scheme on equations (30)-(32) in the t-direction with centering about the mid-point $t^{n+\frac{1}{2}}$ to obtain

$$D_1 U_{r+1}^{n+1} = E_1 U_{r+1}^{n} + K_1, \quad (36)$$
$$D_2 \theta_{r+1}^{n+1} = E_2 \theta_{r+1}^{n} + K_2, \quad (37)$$
$$D_3 \phi_{r+1}^{n+1} = E_3 \phi_{r+1}^{n} + K_3 \quad (38)$$

Subject to the following initial and boundary conditions.

$$u_{r+1}(x_0, t^n) = 1, \quad u_{r+1}(x_{Nx}, t^n) = 0$$
$$\theta_{r+1}(x_0, t^n) = \phi_{r+1}(x_0, t^n) = 1 + \varepsilon e^{nt},$$
$$\theta_{r+1}(x_{Nx}, t^n) = \phi_{r+1}(x_{Nx}, t^n) = 0,$$

Also the initial approximation with reference to the boundary conditions becomes

$$u_{r+1}(y_j, 0) = e^{-y_j}, \quad \theta_{r+1}(y_j, 0) = e^{-y_j} + \varepsilon e^{nt}, \phi_{r+1}(y_j, 0) = e^{-y_j} + \varepsilon e^{nt},$$

where

$$D_1 = \frac{1}{\delta t} - \frac{(a_{0,r} D + a_{1,r} D^2 + a_{3,r})}{2}, \quad E_1 = \frac{1}{\delta t} + \frac{(a_{0,r} D + a_{1,r} D^2 + a_{3,r})}{2}$$
$$D_2 = \frac{Pr}{\delta t} - \frac{(e_{0,r} D + e_{1,r} D^2)}{2}, \quad E_2 = \frac{Pr}{\delta t} + \frac{(e_{0,r} D + e_{1,r} D^2)}{2}$$
$$D_3 = \frac{Sc}{\delta t} - \frac{(f_{0,r} D + D^2 - k\frac{Sc}{2})}{2}, \quad E_3 = \frac{Sc}{\delta t} - \frac{(f_{0,r} D + D^2 - k\frac{Sc}{2})}{2}$$

4. RESULTS AND DISCUSSION

This research article deals with the analysis of unsteady heat and mass transfer of a casson fluid flow. In the formulation of the problem, viscous dissipation, thermal radiation, magnetic field, Soret and Dufour effects were considered in a porous medium. This problem was solved numerically with the help of Spectral Relaxation Method (SRM). SRM involves the use of chebyshev spectral collocation method to solve the system of differential equations. In our computations we set the flow parameters $Gr = 5, Pr = 0.71, Sc = 0.62, Nr = 0.5, A = k_r = \beta = \lambda = 0.5, Gm = 5, M = 0.1, Du = Sr = 0.5, Ec = 0.001$

Hence, all parameters values in this article corresponded to the stated values unless or otherwise defined. Graphs of all relevant flow parameters are presented in figures (2)-(14). By setting the permeability, casson, dufour and soret parameter to be zero $(i.e. \lambda = \beta = Sr = Du = 0)$, our results were the generalized form of Rao et al [21]. Obviously, the results in this article as shown in Table 6 are in good agreement with that of Rao et al [21] when $\lambda = \beta = Sr = Du = 0$

Figure (2) depicted the effect of the thermal buoyancy force parameter (Gr) on the velocity, temperature and concentration profiles. Gr is a dimensionless number that defines the ratio of buoyancy force to the viscous acting on the fluid in the boundary layer thickness. At $Gr = 0$, it means the absence of free convective current. An increase in Gr added more energy into the fluid molecules and loosen up the intermolecular forces within the fluid particles and thereby increasing the velocity profile as shown in figure (2) and the local heat transfer. Figure (3) illustrated the effect of the concentration buoyancy force parameter (Gm) on the velocity, temperature and concentration profiles. It was observed that an increase in Gm brought about increase in the velocity profile.

The influence of the permeability parameter (λ) on the velocity, temperature and concentration profiles was shown in figure (4). It was noticed from figure (4) that the permeability parameter only had influence on the velocity profile. Increasing λ decreased the velocity profile but negligible on the temperature and concentration profiles. Figure (5) also illustrated the effect of the magnetic parameter (M) on the velocity, temperature and concentration profiles. The magnetic field strength β_0 applied transversely to the flow gives rise to an opposing force called Lorentz force. The force had great effect on the velocity equation and it caused a decrease in the velocity profile. This force slowed down the motion of an electrically conducting fluids.

The effect of thermal radiation parameter (Nr) on velocity, temperature and concentration profiles was depicted in figure (6). Thermal radiation had great effect when the fluid temperature was high. When Nr is increased, it enhanced the heat flux from the plate and it was liable to increase the velocity and temperature profiles. This assertion shown in figure (6) as Nr intensified the velocity and temperature profiles. Figure (7) depicted the effect of Prandtl number (Pr) on the velocity, temperature and concentration profiles. It was observed from figure (7) that increase in the Pr caused a decrease in the velocity and temperature profiles. This was because a fluid with higher Pr would have greater viscosities and this reduced the velocities and the skin friction. It was notable that with small values of Pr, the fluid was highly conducive. Figure (8) showed the effect of viscous dissipation expression denoted by the Eckert number (Ec) on the velocity, temperature and concentration profiles. Ec connotes the association between the energy on motion (kinetic energy) in the flow regime and the enthapy. It comprised of the conversion of energy on motion (kinetic energy) into internal energy by work done against the viscous fluid stresses. From figure (8) increase in Ec caused a slight increase in the velocity and temperature profiles.

Figure (9) illustrated the effect of Dufour number (Du) on the velocity, temperature and concentration profiles. It was noticed that increase in Du increased the velocity and temperature profiles. Figure (10) showed the effect of Schmidt number (Sc) on velocity, temperature and concentration profiles. Concentration buoyancy effects frequently delay the progress of fluid velocity. Due to this fact, increase in Sc decreased the velocity and concentration profiles as shown in figure (10). The effect of Soret number (Sr) on the velocity, temperature and concentration profiles was illustrated in figure (11). From figure (11), increase in Sr increased the velocity and concentration profiles. It worth mentioning that, in figures (9) and (10) the effect of Sr and Du alternate each other because a rise in Sr intensify concentration profile while a rise in Du intensify the temperature profile. The plot in figure (12) examined the influence of casson parameter (β) on velocity, temperature and concentration profiles. It was noticeable that increasing β produced a decrease in the fluid velocity because increase in β increased plastic dynamic viscosity which created a retardation in the fluid motion. Figure (13) illustrates the effect of chemical reaction parameter (kr) on the velocity, temperature and concentration profiles. From figure (13) increased in kr decreases the velocity and concentration profiles.

Table 1-6 show the effect of flow parameters such as $\beta, \lambda, Nr, Pr, Gr, Ec$ on the local skin friction, local Nusselt number and local Sherwood number. Table 1 illustrates the effect of β on the local skin friction, local Nusselt number and local sherwood number. We observed from Table 1 that increasing β decreased the local skin friction but has no effect on the local Nusselt number and Sherwood number. In Table 2, the effect of λ on the local skin friction, local Nusselt number and local Sherwood number was illustrated. Table 2 showed that increasing λ decreased the local skin friction. Also, Table 3 illustrates the effect of Nr on the local skin friction, local Nusselt number and local Sherwood number.

Table 3 revealed that when Nr increased, it intensified the local skin friction and reduces the local Nusselt number. Table 4 illustrated the effect of Pr on the local skin friction, local Nusselt number and local Sherwood number. The result in Table 4 revealed that increasing Pr decreased the local skin friction and optimize the local Nusselt number. In Table 5, the effect of Gr while varying Ec is illustrated. Table 5 implies that fixing a value for Gr and varying Ec, the local skin friction is decreasing. Table 6 gives account of the present results compared with Rao *et al* (2013) in the absence of β, λ, Du, Sr (i.e when $\beta = \lambda = Du = Sr = 0$). Our results as shown in Table 6 are in agreement with that of Rao *et al* (2013) when casson parameter, permeability parameter, Dufour and Soret are set to zero. This justifies the solution and the numerical method SRA used in the present study.

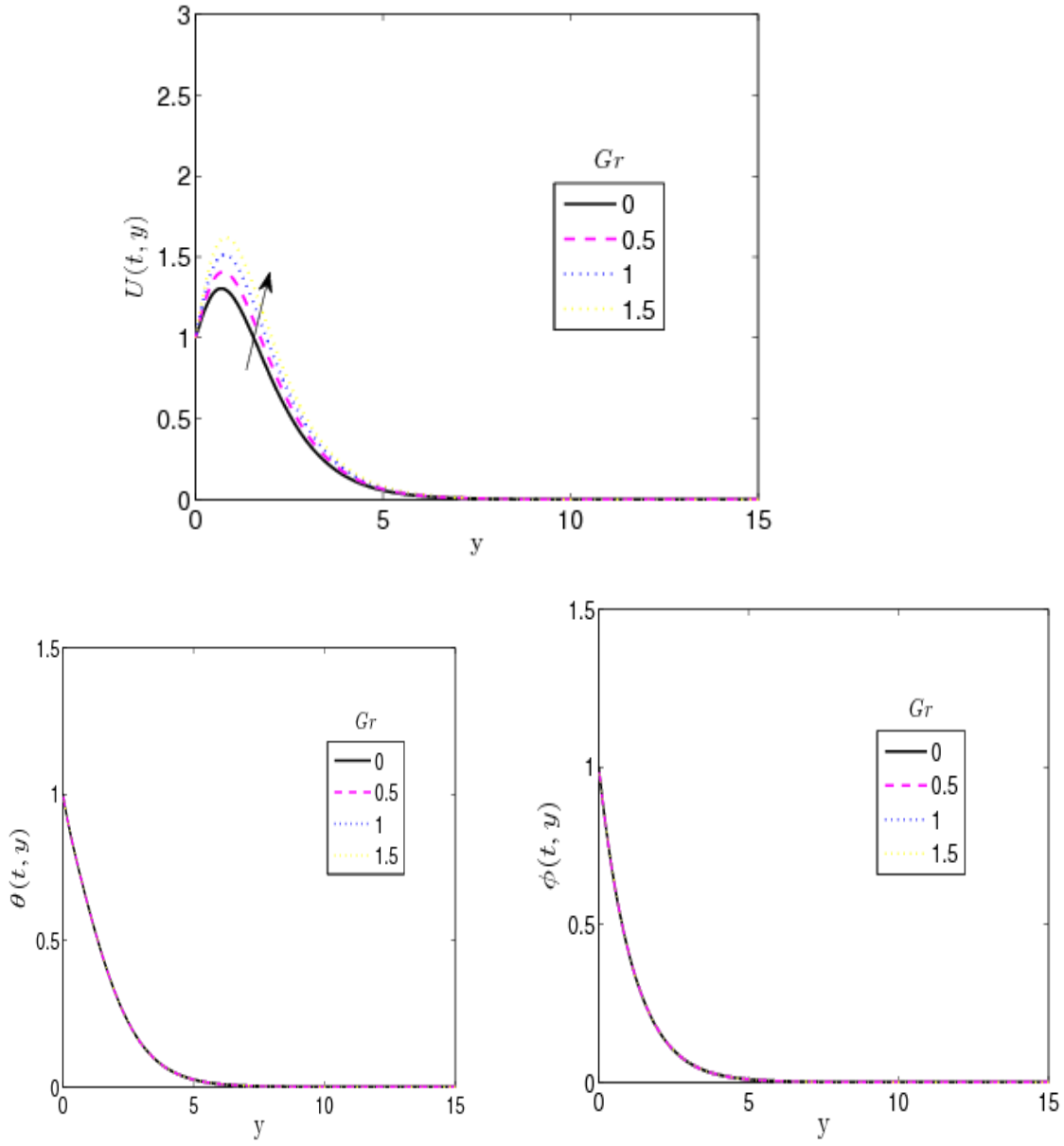

Figure 2: Gr effect on velocity, temperature and concentration profiles

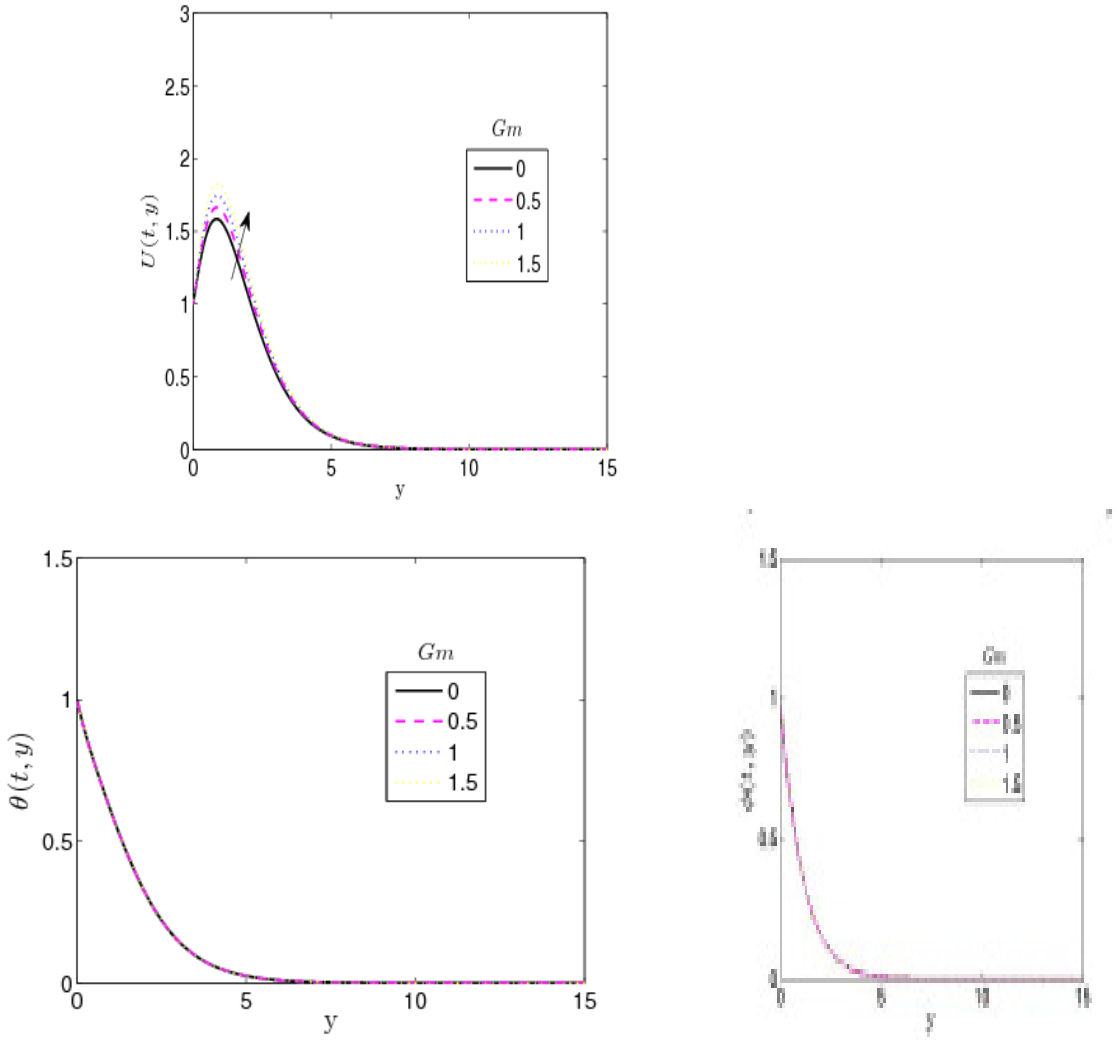

Figure 3: Gm effect on velocity, temperature and concentration profiles

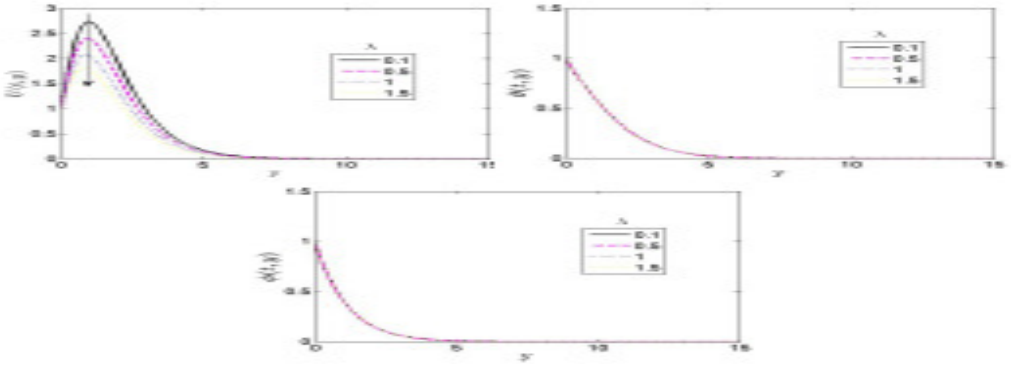

Figure 4: λ effect on velocity, temperature and concentration profiles

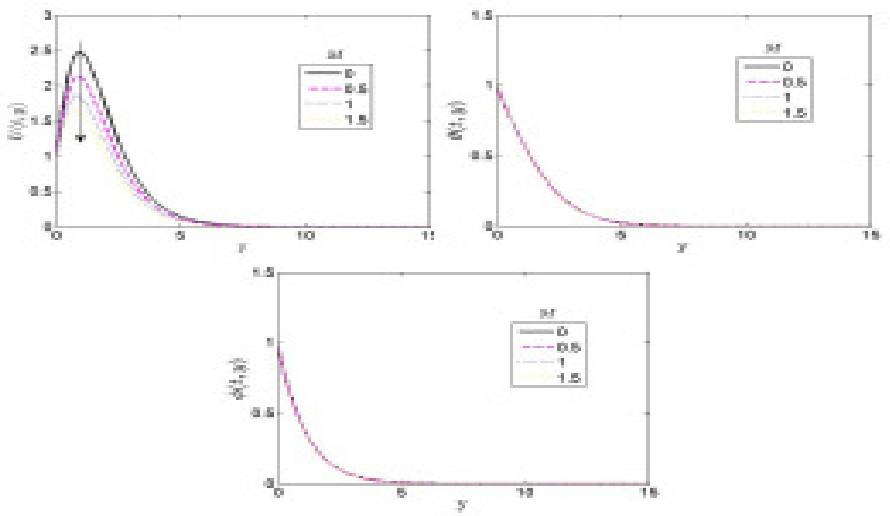

Figure 5: M effect on velocity, temperature and concentration profiles

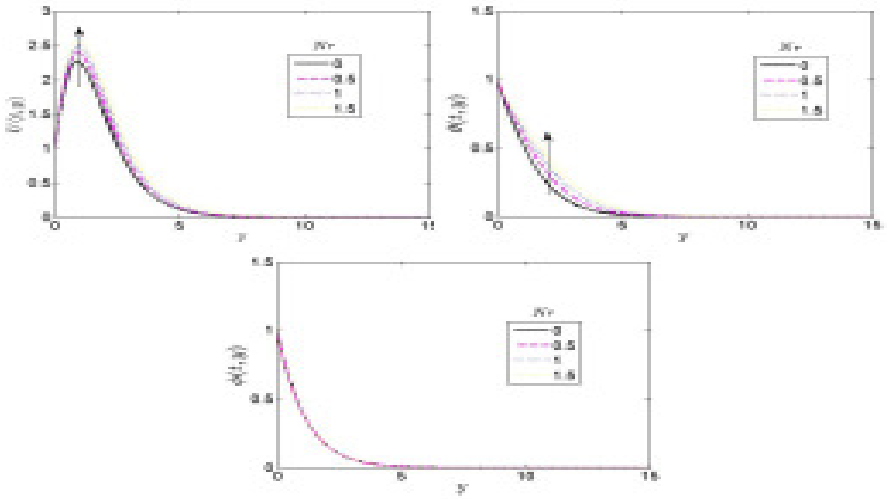

Figure 6: Nr effect on velocity, temperature and concentration profiles

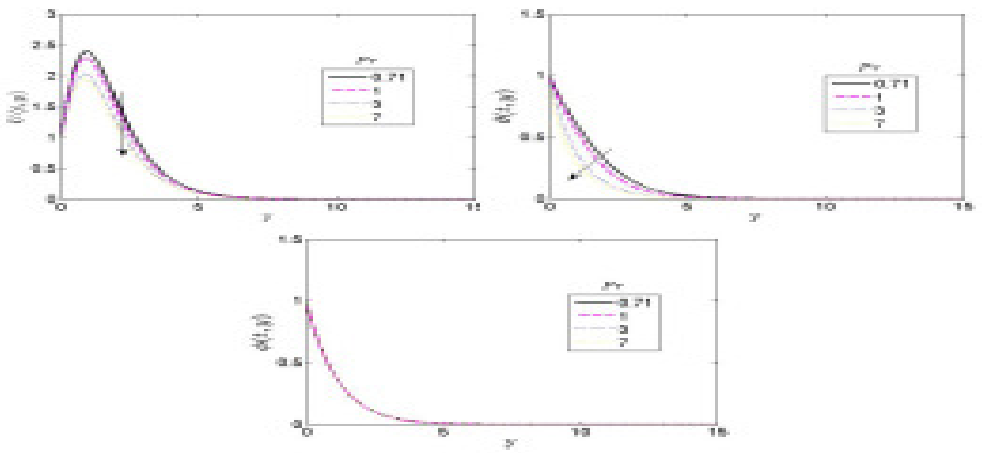

Figure 7: Pr effect on velocity, temperature and concentration profiles

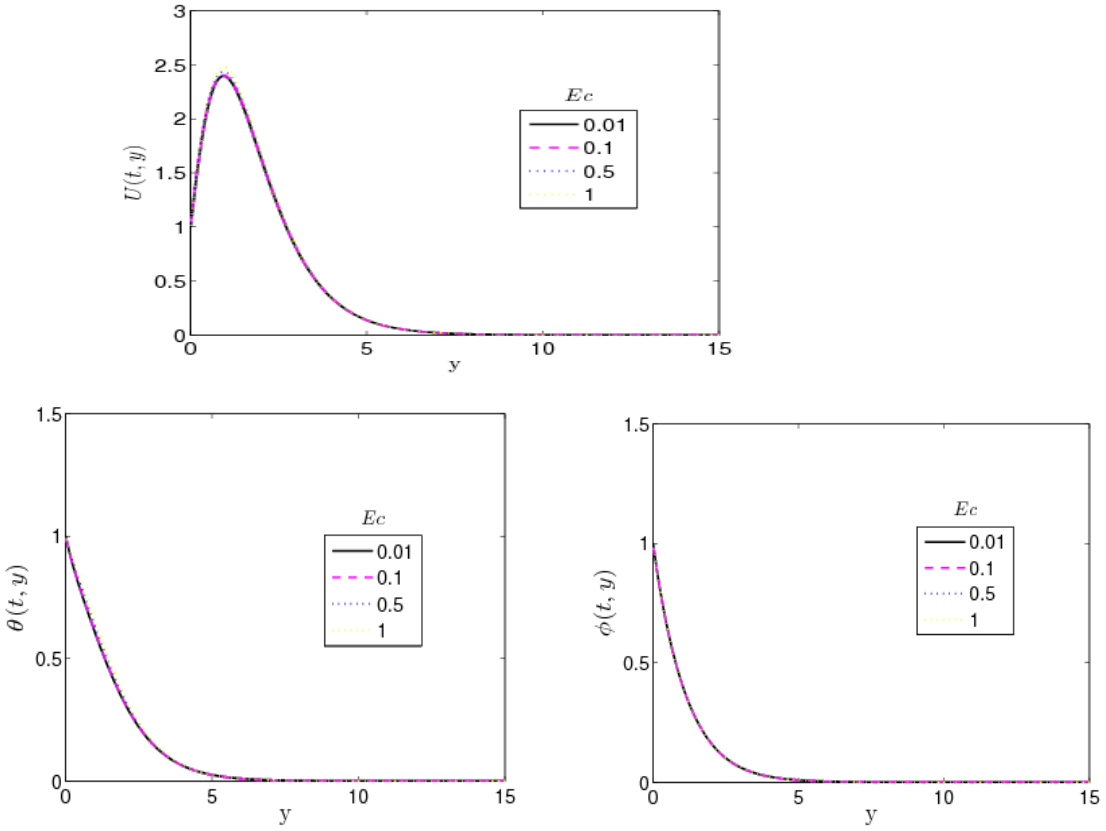

Figure 8: Ec effect on velocity, temperature and concentration profiles

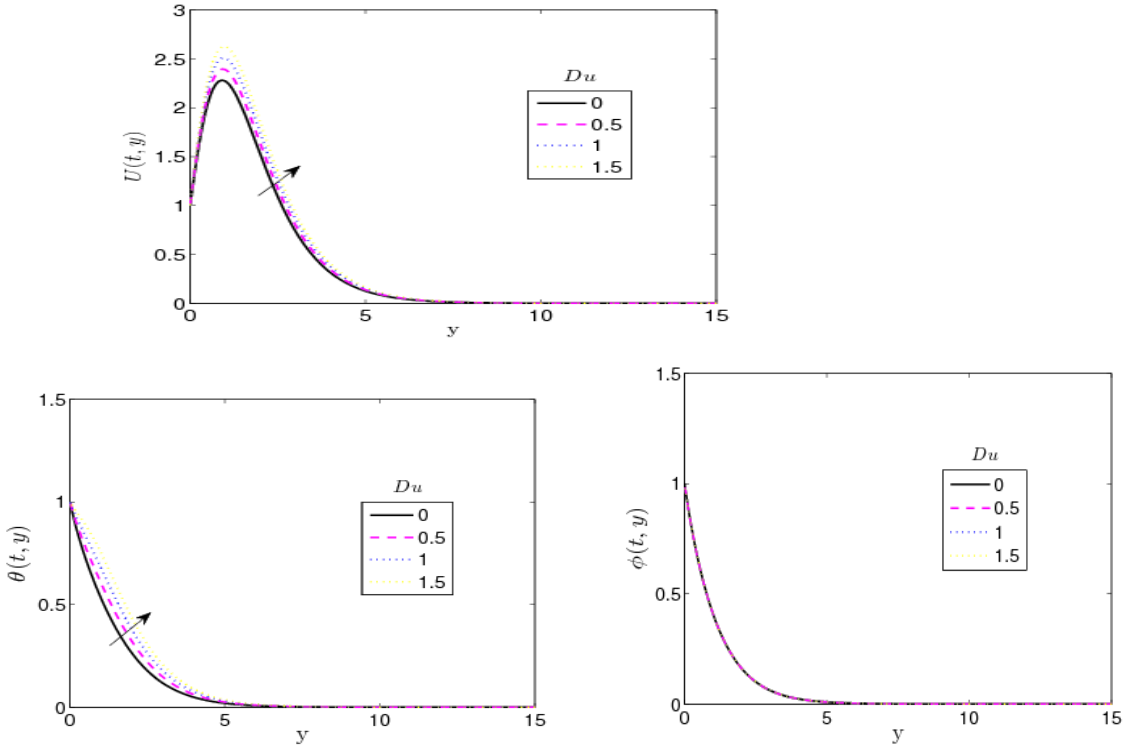

Figure 9: Du effect on velocity, temperature and concentration profiles

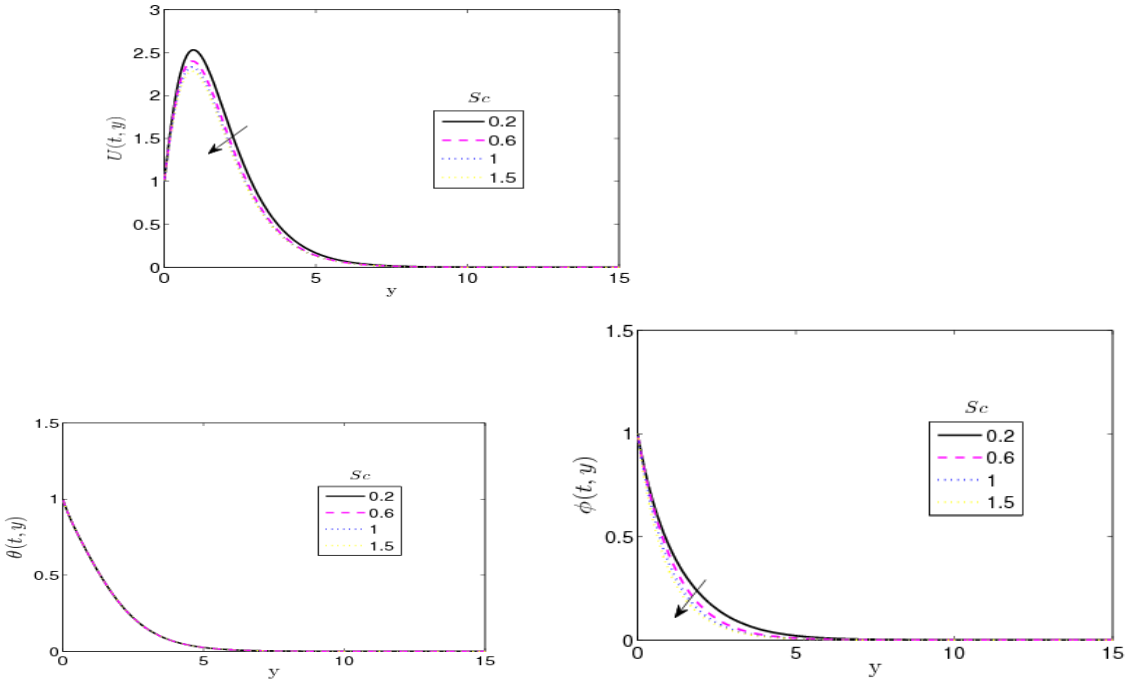

Figure 10: Sc effect on velocity, temperature and concentration profiles

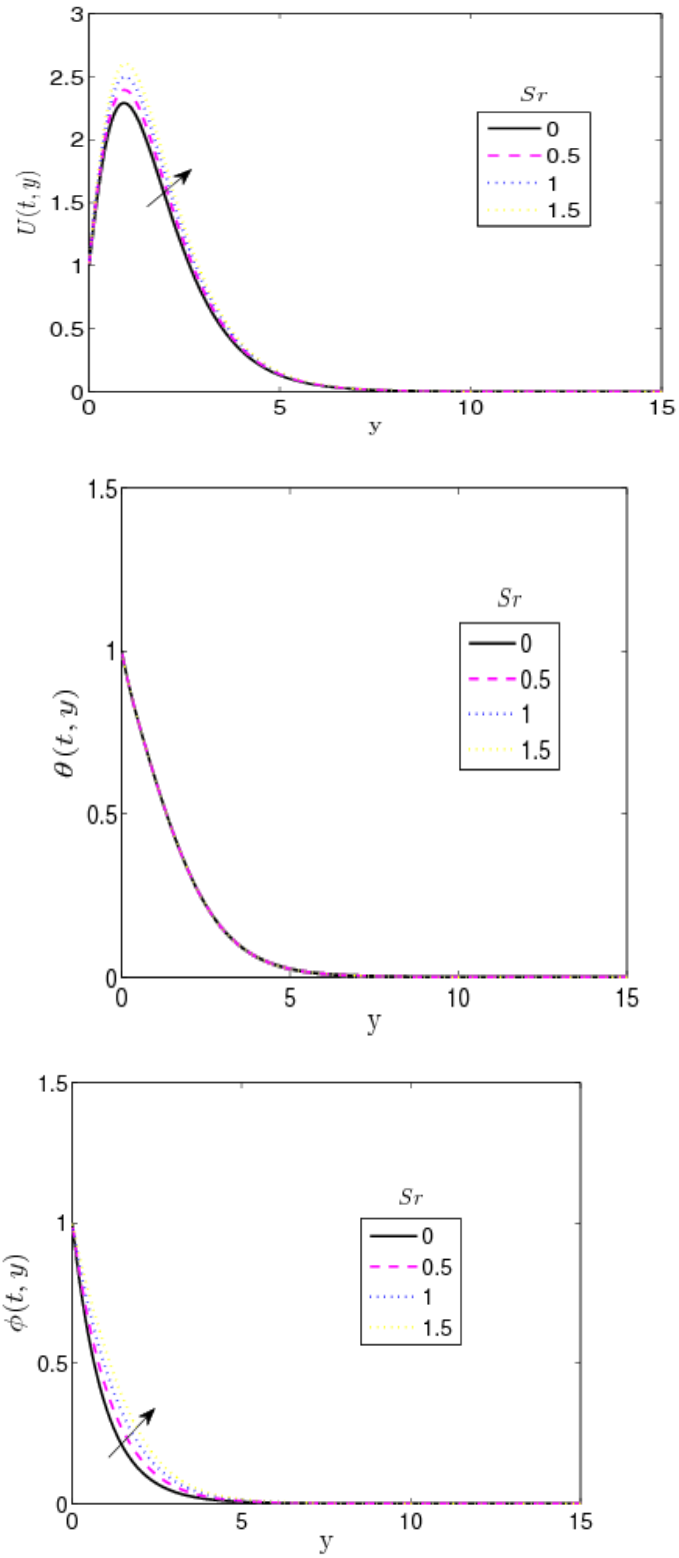

Figure 11: Sr effect on velocity, temperature and concentration profiles

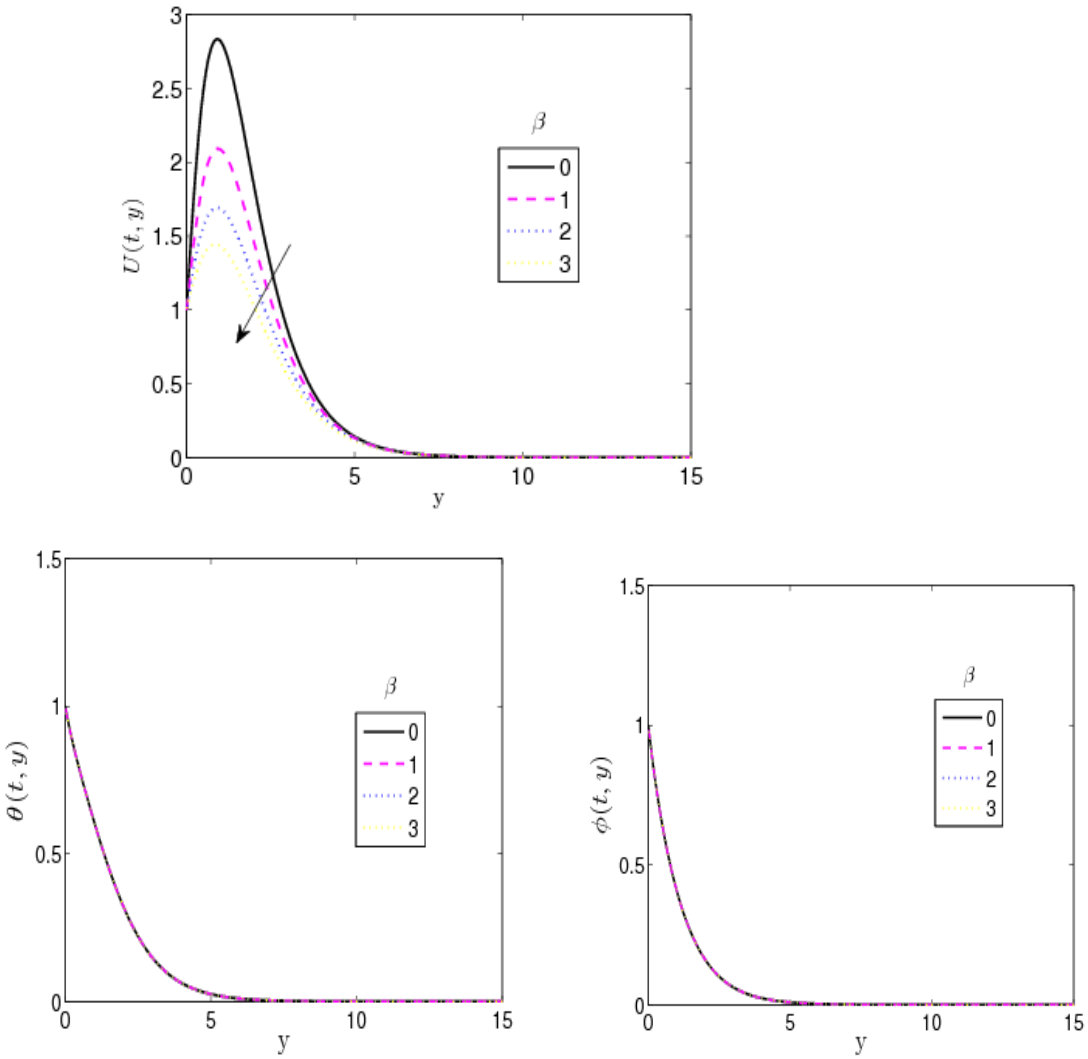

Figure 12: β effect on velocity, temperature and concentration profiles

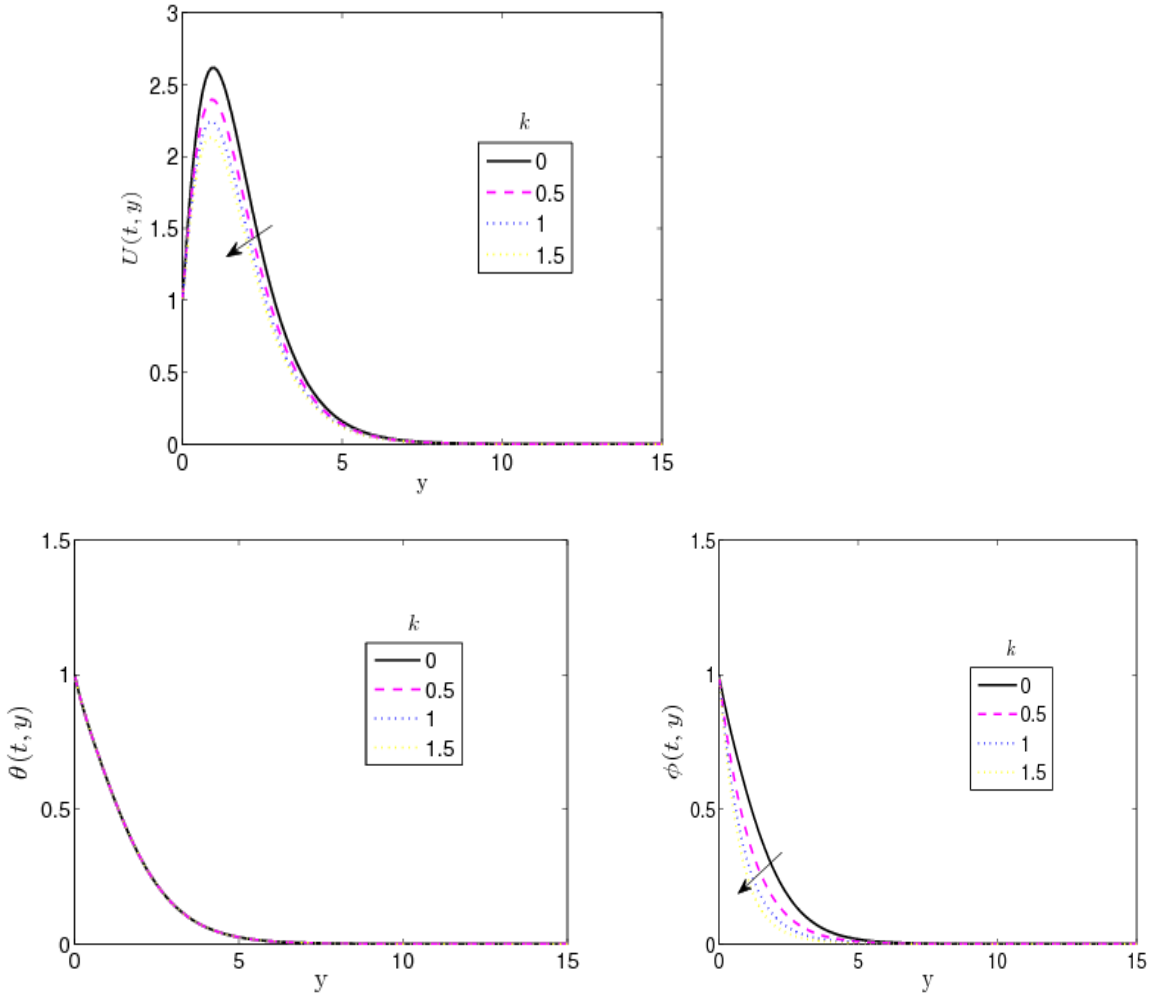

Figure 13: k effect on velocity, temperature and concentration profiles

Table 1: Numerical computations of the local skin friction, local Nusselt number and local Shewrwood number for values of the casson parameter (β) by setting $Gr = 5, Pr = 0.71, Sc = 0.62, Nr = 0.5, A = k_r = \lambda = 0.5, Gm = 5, M = 0.1, Du = Sr = 0.5, Ec = 0.001$

β	$u'(0)$	$-\theta'(0)$	$-\phi'(0)$
0	1.0000	0.5559	0.9100
1.0	0.6480	0.5559	0.9100
2.0	0.6221	0.5559	0.9100
3.0	0.4865	0.5559	0.9100

Table 2: Numerical computations of the local skin friction, local Nusselt number and local Shewrwood number for values of the permeability parameter (λ) by setting $Gr = 5, Pr = 0.71, Sc = 0.62, Nr = 0.5, A = k_r = \beta = 0.5, Gm = 5, M = 0.1, Du = Sr = 0.5, Ec = 0.001$

λ	$u'(0)$	$-\theta'(0)$	$-\phi'(0)$
0.1	0.4604	0.5559	0.9100
0.5	0.2760	0.5559	0.9100
1.0	0.0885	0.5559	0.9100
1.5	0.0632	0.5559	0.9100

Table 3: Numerical computations of the local skin friction, local Nusselt number and local Shewrwood number for values of the thermal radiation parameter (Nr) by setting $Gr = 5, Pr = 0.71, Sc = 0.62, A = k_r = \beta = \lambda = 0.5, Gm = 5, M = 0.1, Du = Sr = 0.5, Ec = 0.001$

Nr	$u'(0)$	$-\theta'(0)$	$-\phi'(0)$
0	0.2149	0.6201	0.9100
0.5	0.2760	0.5559	0.9100
1.0	0.3206	0.5281	0.9100
1.5	0.3555	0.5148	0.9100

Table 4: Numerical computations of the local skin friction, local Nusselt number and local Shewrwood number for values of the Prandtl number (Pr) by setting $Gr = 5, Sc = 0.62, Nr = 0.5, A = k_r = \lambda = 0.5, Gm = 5, M = 0.1, Du = Sr = 0.5, Ec = 0.001$

β	$u'(0)$	$-\theta'(0)$	$-\phi'(0)$
0.71	0.2760	0.5559	0.9100
1.0	0.2242	0.6079	0.9100
3.0	0.0784	0.9993	0.9100
7.0	0.0028	1.7906	0.9100

Table 5: Numerical computations of the local skin friction, local Nusselt number and local Shewrwood number for values of the Eckert number (Ec) and thermal Grashof number (Gr) by setting $Pr = 0.71, Sc = 0.62, Nr = 0.5, A = k_r = \lambda = 0.5, Gm = 5, M = 0.1, Du = Sr = 0.5$

Gr	Ec	$u'(0)$	$-\theta'(0)$	$-\phi'(0)$
0.0	0	0.4228	0.5547	0.9100
	0.1	0.4228	0.5432	0.9100
	0.5	0.4228	0.4917	0.9100
	1.0	0.4228	0.4274	0.9100
0.5	0	0.3459	0.5547	0.9100
	0.1	0.3454	0.5432	0.9100
	0.5	0.3432	0.4917	0.9100
	1.0	0.3404	0.4274	0.9100
1.0	0	0.2829	0.5547	0.9100
	0.1	0.2820	0.5432	0.9100
	0.5	0.2780	0.4917	0.9100
	1.0	0.2301	0.4274	0.9100
1.5	0	0.2130	0.5547	0.9100
	0.1	0.2117	0.5432	0.9100
	0.5	0.2056	0.4917	0.9100
	1.0	0.1981	0.4274	0.9100

Table 6: Comparison of Numerical computations for skin-friction coefficient Cf and Sherwood number $Nu_x Re_x^{\frac{1}{2}}$ for various values of Schmidt number (Sc) compared with Rao et al.[21] when $Gr = 5, Pr = 0.71, Nr = 0.5, A = k_r = 0.5, \beta = \lambda = Sr = Du = 0, Gm = 5, M = 0.1, Du = Sr = 0.5, Ec = 0.001$

.

		Present Study		Rao et al.[21]
R	Cf	$-\phi'(0)$	Cf	$-\phi'(0)$
0.22	3.1092	0.4534	3.1068	0.4515
0.60	2.4656	0.8453	2.4548	0.8431
0.78	2.2782	1.0232	2.2767	1.0214
0.94	2.1542	1.1754	2.1540	1.1745

5. CONCLUSION AND REMARKS

In this article, the problem of unsteady casson fluid flow past a semi-infinite vertical plate embedded in a porous medium is solved with a novel numerical method namely spectral relaxation method (SRM). Spectral methods are known for their accuracy and easy computations. The result obtained with SRM is compared with existing result in literature and it is found to be in good agreement.

Conclusions drawn from the study are as highlighted below;

- The permeability parameter (λ) decreases the velocity profile when it is increased
- Increasing the magnetic parameter decreases the velocity profile due to the applied magnetic field strength (β_0)
- The dufour number increases the velocity and temperature profiles when it is increased.
- Increasing the Soret number increases the velocity and concentration profiles respectively. It is noticed that the influence of soret and dufour is opposite.
- Increasing the casson parameter (β) reduces the local skin friction but has no effect on the local Nusselt number and local sherwood number.

REFERENCES

1. Adegbie, K.S and Fagbade, A.I (2015). Influence of Variable fluid properties and radiative heat loss on magnetohydrodynamics forced convection flow in a fluid saturated porous medium. Journal of Nigerian Association of Mathematical Physics, 30:101-16.
2. Alao, F.I., Fagbade, A.I., Falodun, B.O. (2016). Effects of thermal radiation, soret and Dufour on an unsteady heat and mass transfer flow of a chemically reacting fluid past a semi-infinite vertical plate with viscous dissipation. Journal of the Nigeria Mathematical Society, 35:142-158.
3. Animasaun I.L. (2015). Effects of thermophoresis, variable viscosity and thermal conductivity on free convective heat and mass transfer on non-darcian MHD dissipative casson fluid flow with suction and n^{th} order of chemical reaction. Journal of the Nigerian Mathematical Society, 34:11-31.
4. Animasaun I.L., Adebile E.A., Fagbade A.I. (2016).Casson flow with variable thermo-physical property along exponentially stretching sheet with suction and exponentially decaying internal heat generation using the homotopy analysis method. Journal of the Nigerian Mathematical Society, 35:1-17.
5. Bhavana, M., Chenna kesavaiah, D., Sudhakaraiah, A (2013). The soret effect on free convective unsteady MHD flow over a vertical plate with heat source. International Journal of Innovative Research in Science, Engineering and Technology, 2(5):1617-1628.
6. Emmanuel, M.A., Ibrahim, Y.S, Letis, B.B. (2015). Analysis of casson fluid flow over a vertical porous surface with chemical reaction in the presence of magnetic field. Journal of Applied Mathematics and Physics, 3:713-723.
7. Falodun, B. O and Amoo, S. A. (2017). Spectral Relaxation Analysis of Unsteady Casson Fluid Flow Past a Semi- infinite Vertical Porous Plate Under the influence of Thermo-diffusion and Diffusion-thermo. In 28th Annual Colloquium and Congress of Nigeria Association of Mathematical Physics, Bayero University Kano, Kano Nigeria. 31st October to 3rd November, 2017
8. Hayat, T., Shehzadi, S.A., Alsaedi, A (2012). Soret and Dufour effects on magnetohydrodynamics (MHD) flow of Casson fluid. Appl. Math. Mech (English Ed.), 33(10): 1301-1312.
9. Kishore, P.M., Vijaya Kumar, S. Varma, Masthan Rao, S. and Bala Murugan, K.S (2014). The effect of chemical reaction on MHD free convective flow of dissipative fluid past an exponentially accelerated vertical plate. International Journal of Computational Engineering Research, 4(1):11-26.
10. Kumaran G., Sandeep N., Ali M.E. (2017). Computational analysis of magnetohydrodynamics casson and Maxwell flows over a stretching sheet with cross diffusion. Results in Physics, 7:147-155.
11. Masthan Rao, S. Balamurugan, K.S., Varma, S. V.K., Raju, V.C.C (2013). Chemical reaction and Halls effects on MHD convective flow along an infinite vertical porous plate with variable suction and heat absorption. Applications and Applied Mathematics: An International Journal, 8(1):268-288.
12. Mohammed, I.S. and Suneetha, K (2016). Influence of thermo-diffusion and heatsource on MHD free convective reacting fluid flow in a porous vertical surface. Journal of Advances in Applied Mathematics, 1(1);17-28.
13. Monica Medikare, Sucharitha Joga, Kishore Kumar Chiderm (2016). MHD stagnation point flow of a casson fluid over a Nonlinear stretching sheet with viscous dissipation. American Journal of Computational Mathematics, 6: 37-48.
14. Motsa, S. S, Dlamini, P. G and Khumalo, M. (2013). A new multistage spectral relaxation method for solving chaotic initial value system.Nonlinear Dynamics, (7291):265-83.
15. Muhammad A Imran, Skakila Sarwar and Muhammad Imran (2016). Effects of slip on free convective flow of Casson fluid over an oscillating vertical plate. Boundary Value Problems, 30:1-11.

16. Prakash jagdish, K.S. Balamurugan and Varma, S. Vijaya Kumar (2015). Thermo-diffusion and Chemical reaction effects on MHD three dimensional free convective couette flow. Walailak Journal Science and Technology, 12(9):805-830.
17. Pramanik, S (2014). Casson fluid flow and heat transfer past an exponentially porous stretching surface in presence of thermal radiation. Ain Shams Engineering Journal, 5:205-212.
18. Pushpalatha K., Ramana Reddy, J.V., Sugunamma, V. and Sandeep, N (2017). Numerical study of chemically reacting unsteady casson fluid flow past a stretching surface with cross diffusion and thermal radiation. De Gruyter Open, 7:69-76.
19. Rallabandi Srinivasa Raju (2016). Combined influence of thermal diffusion and diffusion thermo on unsteady MHD free convective fluid flow past an infinite vertical porous plate in presence of chemical reaction. J. Inst. Eng. India Ser., 97(4):505-515.
20. Rao, V.S, Baba, L.A, Raju, R.S (2013). Finite element analysis of radiation and mass transfer flow past semi-infinite moving vertical plate with viscous dissipation. Journal of Applied Fluid Mechanics, 6:321-329.
21. Shivaiah, S. and Anand J. Rao(2012). Chemical reaction effect on an unsteady MHD free convection flow past a vertical porous plate in the presence of suction or injection. Theoretical Application Mechanics, 39(2);185-208.
22. Srinivasa R. Raju (2016). Numerical treatment of casson fluid free convective flow past an infinite vertical plate filled in magnetic field in presence of thermal radiation: A finite element techniques. International Journal of Engineering and Applied Sciences, 4:119-133.
23. Sulochana, C., Ashwinkumar, G.P. and Sandeep, N (2016). Numerical Investigation of chemically reacting MHD flow due to a rotating cone with thermophoresis and Brownian motion. International Journal of Advanced Science and Technology, 86:61-74.
24. Vidyasagar, B., Raju, M.C and Varma, S.V.K (2015). Unsteady MHD free convection flow of a viscous dissipative Kuvshinski fluid past an infinite vertical porous plate in the presence of radiation, thermal diffusion and chemical effects. Journal of Applied and Computational Mathematics, 4(5):1-11.
25. Yanala D.R. and Vempati S.R.(2016). Numerical solution of thermo-diffusion and diffusion-thermo effects on unsteady MHD free convective mass transfer flow past an infinite vertical porous plate with oscillatory suction velocity. International Journal of Multidicipline Research and Advances in Engineering, 8(2):15-37.